Electronic Supplementary Information

The Nature of Interactions of Benzene with CF_3I and CF_3CH_2I

Maciej Bujak[a,b,]*, Hans-Georg Stammler[b], Sebastian Blomeyer[b],
and Norbert W. Mitzel[b,]*

[a]Faculty of Chemistry, University of Opole, Oleska 48, 45-052 Opole, Poland; E-mail: mbujak@uni.opole.pl
[b]Lehrstuhl für Anorganische Chemie und Strukturchemie and Centrum für Molekulare Materialien CM_2, Fakultät für Chemie Universität Bielefeld; Lehrstuhl für Anorganische Chemie und Strukturchemie, Fakultät für Chemie, Universität Bielefeld, Universitätsstraße 25, 33615 Bielefeld, Germany; E-mail: mitzel@uni-bielefeld.de

Table of Contents

Materials and Experimental Procedures

The commercially available trifluoroiodomethane, CF_3I, (**1**) 1,1,1-trifluoro-2-iodoethane, CF_3CH_2I (**3**) and benzene, C_6H_6, were used, without further purification, in the *in-situ* low-temperature crystallization and co-crystallization experiments. The single crystal samples of $(CF_3I)_2{\cdot}C_6H_6$ (**2**) and $CF_3CH_2I{\cdot}C_6H_6$ (**4**) were successfully co-crystallized from the mixtures of halogenated coformers with benzene in the molar ratio of *ca.* 2:1 and 5:1, respectively. It is noteworthy that the 2:1 molar ratio mixture of $CF_3CH_2I{:}C_6H_6$ led to crystallization of C_6H_6 coformer.[1]

A general experimental procedure of the *in-situ* low-temperature crystallization was previously reported.[2] All the samples *i.e.* **1** and **3** and their mixtures with C_6H_6 were loaded (cryogenically, employing Schlenk technique, in the case of CF_3I and its mixture with C_6H_6) in thin-walled glass capillaries of the 0.3–0.4 mm internal diameter. The liquid samples, filling *ca.* 15–20 mm of the sealed capillaries, were cooled on the diffractometer, in a nitrogen gas stream from an Oxford Cryosystems attachment. At the first stage the samples froze as the milky polycrystalline materials, which then were slowly warmed, at the rate of 0.2–1.0 K/h, close to their melting points reducing the number of crystal grains. At the next stage by manual local warming, using a steel wire from a paper clip, monitored under a microscope followed by slow temperature lowering (rate of 1-2 K/h), it was possible to grow sufficiently large single crystals and co-crystals of all the samples. The first data sets were collected at the highest temperatures determined by melting points or phase transition temperatures, and then at 100.0(1) K. The first data collection for **4** co-crystal (melting point of 196(1) K) was undertaken at 160.0(1) K because the material fully filling the capillary was frozen only at *ca.* 165 K.

The low-temperature diffraction data were collected on SuperNova diffractometer, with the graphite monochromated MoKα radiation (λ = 0.71073 Å). The reflections were measured using ω-scan technique with $\Delta\omega$ = 1.0° and 8.0 s exposure time. All data were accounted for the Lorentz, polarization and sample absorption effects.[3] The structures were solved by direct methods and refined with SHELX.[4]

The simulated powder diffraction diagrams[5] for the high-temperature phases of **1** at 120 K (a) and **2** at 140 K (c) along with the experimental X-ray powder diffraction patterns[3] for their low-temperature phases at 95 K (b) and 120 K (d), respectively, are depicted in Figure S1.

The calculated difference Fourier maps revealed a dynamic disorder of, sitting on a mirror plane, the $–CF_3$ groups in the structures of **1** and **2**. The disorder is realized by the presence of two positions for all the fluorine atoms (Figure S2). The occupation factors for two components of the split $–CF_3$ groups were refined using dependent free variables until converged at 78% (F11 and F21) and 22% (F12 and F22) for **1**, and at 65% (F11 and F21) and 35% (F12 and F22) for **2**. The disordered parts were treated using appropriate geometrical restraints.[4] The disorder of CF_3CH_2I molecules in **4** is about a special position (mirror plane). In contrast to the CF_3I disorder, it could be considered as a static in nature. The same crystallographic position is statistically occupied by two CF_3CH_2I molecules assuming opposite orientations, related by mirror symmetry. As a result the disordered molecules with two mutually, superimposed, interchangeable -CF_3 and -I substituents are observed (Figure S3).

The carbon, fluorine and iodine atoms, in all the studied crystal and co-crystal structures, were refined with anisotropic displacement parameters. All the hydrogen atoms were located in the subsequent difference Fourier maps. The H-atoms were refined using geometrical restraints (SADI and DFIX command of SHELXL[4]). The hydrogen-atom displacement parameters were taken with coefficient being 1.2 times larger than the respective equivalent isotropic parameters of their carrier carbon atoms. The CrysAlisPro program[3] was used for the data collection, unit-cell refinement and data reduction. The crystal data and structure determination summary are listed in Table S1. The bond lengths, angles and the shortest intermolecular distances are gathered in Tables S2-S4. The intermolecular contacts were compared using the Hirshfeld surface analysis provided by CrystalExplorer 2.0.[6]

The structure drawings were prepared using Mercury.[5] Figures S4 and S5 show the packing diagrams along with the accessible intermolecular space of **1** and **2** as well as of **3** and **4**, respectively.

The geometry optimizations and the subsequent calculations on **1**, **2**, **3** and **4** were run using the Gaussian 09 program package[7] along with GaussView 5.0 software as a graphical interface.[8] The DFT calculations were performed at the B3LYP/3–21G* and B3LYP/6–311G** (partial atomic charges, NBO)[9-12] level of theory, in vacuum, for the geometries obtained from the X-ray diffraction experimental results as an input (only one, dominant occupied positions of the disordered molecules were considered). The molecular isodensity surfaces, color-coded according to the calculated local electrostatic potential are depicted in Figure S6.

The conformational landscape was explored with the help of Grimme's gfn2-xtb method.[14] The structures obtained herein were further optimised on M06-2X/def2TZVP level of theory, followed by single-point calculations on B2PLYPD3/def2QZVP level of theory, using Gaussian 16, Revision B.01.[15] NBO analyses were performed using the interface with NBO3 implemented in Gaussian.[16] SAPT0 analyses were carried out based on the optimised structures mentioned above and using the PSI4 program code and def2TZVP basis sets.[17] All energies obtained in these calculations are listed in Tables S5-S7; Cartesian coordinates of all species can be found in Tables S8-S13.

Table S1: The low-temperature crystal data and structure determination summary for **1**, **2**, **3** and **4**.

	CF_3I, **1**	$(CF_3I)_2{\cdot}C_6H_6$, **2**	CF_3CH_2I, **3**	CF_3CH_2I, **3**	$CF_3CH_2I{\cdot}C_6H_6$, **4**	$CF_3CH_2I{\cdot}C_6H_6$, **4**
formula	CF_3I	$C_8H_6F_6I_2$	$C_2H_2F_3I$	$C_2H_2F_3I$	$C_8H_8F_3I$	$C_8H_8F_3I$
fw, g/mol	195.91	469.93	209.94	209.94	288.04	288.04
crystal size, mm	0.3 x 0.2 x 0.2	0.3 x 0.3 x 0.2	0.2 x 0.2 x 0.1	0.2 x 0.2 x 0.1	0.03 x 0.03 x 0.02	0.03 x 0.03 x 0.02
crystal system	orthorhombic	monoclinic	tetragonal	tetragonal	orthorhombic	orthorhombic
space group, Z, Z'	*Cmce*, 8, 0.5	$C2/m$, 2, 0.25	$I4_1/a$, 16, 1	$I4_1/a$, 16, 1	*Cmcm*, 4, 0.25	*Cmcm*, 4, 0.25
temperature, K	120.0(1)	140.0(1)	185.0(1)	100.0(1)	160.0(1)	100.0(1)
a, Å	7.5125(3)	8.7050(5)	20.4193(2)	20.2203(3)	11.7746(7)	11.6928(5)
b, Å	5.8369(2)	8.7152(4)	20.4193(2)	20.2203(3)	7.8765(7)	7.8172(5)
c, Å	19.3089(7)	9.7655(6)	4.7907(2)	4.7384(2)	11.2397(9)	11.1700(7)
β, °	90	110.146(7)	90	90	90	90
V, Å^3	846.69(5)	695.54(7)	1997.47(9)	1937.35(10)	1042.40(14)	1020.99(10)
ρ, g/cm^3	3.074	2.244	2.792	2.879	1.835	1.874
μ, mm^{-1}	7.461	4.562	6.335	6.532	3.063	3.127
θ range, °	2.1 - 26.0	3.4 - 26.0	2.0 - 25.9	2.0 - 26.0	3.1 - 26.0	3.1 - 26.0
index ranges	$-9 \le h \le 9$	$-10 \le h \le 10$	$-25 \le h \le 25$	$-24 \le h \le 24$	$-14 \le h \le 14$	$-14 \le h \le 14$
	$-7 \le k \le 7$	$-10 \le k \le 10$	$-25 \le k \le 25$	$-24 \le k \le 24$	$-9 \le k \le 9$	$-9 \le k \le 9$
	$-23 \le l \le 23$	$-12 \le l \le 12$	$-5 \le l \le 5$	$-5 \le l \le 5$	$-13 \le l \le 13$	$-13 \le l \le 13$
reflns collected	9884	5814	15467	14784	8770	8489
R_{int}	0.0577	0.0780	0.0319	0.0387	0.0590	0.0595
data [$I > 2\sigma(I)$]	448	696	961	949	500	511
data/parameters	450/45	729/63	970/62	949/62	570/53	557/52
GOF on F^2	1.096	1.145	1.298	1.409	1.114	1.091
R_1 [$I > 2\sigma(I)$]	0.0383	0.0334	0.0209	0.0229	0.0244	0.0203
R_1 (all data)	0.0385	0.0344	0.0212	0.0229	0.0298	0.0234
wR_2 (all data)	0.0893	0.0847	0.0461	0.0520	0.0614	0.0473
lrgst diff peak, e/Å^3	1.445	1.072	0.477	0.856	0.193	0.256
lrgst diff hole, e/Å^3	–0.860	–0.554	–0.312	–0.474	–0.177	–0.207
CCDC number	1873282	1873283	1873284	1873285	1873286	1873287

Table S2: The molecular dimensions (Å, °) for **1**, **2**, **3** and **4**.

Compound	**1**	**2**	Compound	**3**	**3**		**4**	**4**
Temperature, K	120	140	Temperature, K	185	100		160	100
C1–I1	2.126(13)	2.099(9)	C1–F1	1.326(4)	1.327(5)	C1–F1	1.323(14)	1.357(10)
C1–F11	1.379(14)	1.283(11)	C1–F2	1.327(4)	1.342(5)	C1–F2/F2^{IV}	1.347(8)	1.339(6)
C1–F12	1.40(3)	1.247(18)	C1–F3	1.341(4)	1.350(5)			
C1–F21/F21$^{I/II}$	1.268(9)^{I}	1.332(8)^{II}	C1–C2	1.489(5)	1.490(6)	C1–C2	1.486(13)	1.480(11)
C1–F22/F22$^{I/II}$	1.32(3)^{I}	1.302(14)^{II}	C2–I1	2.134(4)	2.139(4)	C2–I1	2.075(2)	2.0844(19)
I1–C1–F11	106.9(9)	115.0(7)	F1–C1–F2	107.6(3)	107.5(4)	F1–C1–F2/F2^{IV}	106.4(8)	105.2(6)
I1–C1–F12	101.1(18)	113.9(12)	F1–C1–F3	107.1(3)	107.0(3)	F2–C1–F2^{IV}	106.0(10)	105.5(8)
I1–C1–F21/F21$^{I/II}$	111.8(7)^{I}	112.0(5)^{II}	F2–C1–F3	106.1(3)	105.9(4)			
I1–C1–F22/F22$^{I/II}$	121.9(16)^{I}	109.1(8)^{II}	F1–C1–C2	110.3(3)	110.7(4)	F1–C1–C2	113.2(8)	112.1(7)
F11–C1–F21/F21$^{I/II}$	105.2(7)^{I}	107.0(6)^{II}	F2–C1–C2	113.1(3)	112.8(4)	F2/F2^{IV}–C1–C2	112.1(7)	114.0(5)
F21–C1–F21$^{I/II}$	115.1(11)^{I}	103.1(8)^{II}	F3–C1–C2	112.4(3)	112.7(4)			
F12–C1–F22/F22$^{I/II}$	100.5(16)^{I}	110.0(9)^{II}	C1–C2–I1	112.4(3)	112.3(3)	C1–C2–I1	114.2(5)	112.9(4)
F22–C1–F22$^{I/II}$	106(2)^{I}	104.4(13)^{II}	F1–C1–C2–I1	176.6(2)	176.5(3)	F1–C1–C2–I1	180.0	180.0
			F2–C1–C2–I1	–62.8(4)	–63.1(4)	F2–C1–C2–I1	–59.6(7)	–60.6(6)
			F3–C1–C2–I1	57.2(4)	56.8(4)	F2^{IV}–C1–C2–I1	59.6(7)	60.6(6)
			C2–H21	0.93(3)	0.94(4)	C2–H2/H2^{V}	0.98(2)	0.98(2)
			C2–H22	0.94(3)	0.95(4)			
			C1–C2–H21	111(3)	111(3)	C1–C2–H2/H2^{V}	108.9(8)	109.6(7)
			C1–C2–H22	110(3)	109(3)			
			I1–C2–H21	106(3)	106(3)	I1–C2–H2/H2^{V}	109.3(7)	109.1(7)
			I1–C2–H22	107(3)	109(3)			
			H21–C2–H22	111(4)	109(5)	H2–C2–H2^{V}	106(3)	106(3)
C2–C2^{II}		1.375(13)				C3–C4/C4^{IV}	1.369(3)	1.377(2)
C2/C2^{III}–C3		1.383(8)				C4–C4^{I}	1.368(5)	1.372(4)
C2–H2		0.92(6)				C3–H3	0.95(3)	0.94(2)
C3–H3		0.92(6)				C4–H4	0.97(2)	0.95(2)
C2–C3–C2^{III}		119.4(8)				C3–C4–C4^{I}	120.09(16)	120.04(14)
C2^{II}–C2–C3		120.3(4)				C4–C3–C4^{VI}	119.8(3)	119.9(3)
C2^{I}–C2–H2		116(4)				C3–C4–H4	119.5(15)	120.5(13)
C2/C2^{III}–C3–H3		120.3(4)				C4/C4^{VI}–C3–H3	120.09(16)	120.04(14)
C3–C2–H2		124(5)				C4^{I}–C4–H4	120.4(15)	119.5(13)
C2^{II}–C2–C3–C2^{III}		0.0				C4^{VI}–C3–C4–C4^{I}	0.0	0.0

Symmetry codes: (I) *–x*, *y*, *z*; (II) *x*, *–y*, *z*; (III) *–x* + 1, *y*, *–z*; (IV) *x*, *y*, *–z* + 1/2; (V) *–x*, *y*, *–z* + 1/2; (VI) *x*, *–y* + 1, *–z* + 1.

Table S3: The dimensions (Å, º) of the intermolecular interactions in **1** and **2**.

Compound Temperature, K	**1** 120	Compound Temperature, K	**2** 140
I1···I1$^{\mathrm{I}}$	3.9284(10)	I1···C2	3.632(7)
C1–I1···I1$^{\mathrm{I}}$	167.1(3)	C1–I1···C2	168.50(12)
I1···I1$^{\mathrm{I}}$–C1$^{\mathrm{I}}$	97.0(3)	I1···C2–C2$^{\mathrm{VII}}$	79.09(10)
		I1···C2–C3	85.4(3)
C1–I1···I1$^{\mathrm{I}}$–C1$^{\mathrm{I}}$	180.0	C1–I1···C2–C2$^{\mathrm{VII}}$	161.4(11)
		C1–I1···C2–C3	–76.6(12)
I1···I1$^{\mathrm{II}}$	3.9284(10)	I1···C2$^{\mathrm{VII}}$	3.632(7)
C1–I1···I1$^{\mathrm{II}}$	97.0(3)	C1–I1···C2$^{\mathrm{VII}}$	168.50(12)
I1···I1$^{\mathrm{II}}$–C1$^{\mathrm{II}}$	167.1(3)	I1···C2$^{\mathrm{VII}}$–C2	79.09(10)
		I1···C2$^{\mathrm{VII}}$–C3$^{\mathrm{VIII}}$	85.4(3)
C1–I1···I1$^{\mathrm{II}}$–C1$^{\mathrm{II}}$	180.0	C1–I1···C2$^{\mathrm{VII}}$–C2	–161.4(11)
		C1–I1···C2$^{\mathrm{VII}}$–C3$^{\mathrm{VIII}}$	76.6(12)
F12···F12$^{\mathrm{III}}$	2.30(7)		
C1–F12···F12$^{\mathrm{III}}$	175(4)		
F12···F12$^{\mathrm{III}}$–C1$^{\mathrm{III}}$	175(4)		
C1–F12···F12$^{\mathrm{III}}$–C1$^{\mathrm{III}}$	180.0		
F21···F21$^{\mathrm{IV}}$	2.781(16)	F22···F22$^{\mathrm{IX}}$	2.51(3)
C1–F21···F21$^{\mathrm{IV}}$	157.9(7)	C1–F22···F22$^{\mathrm{IX}}$	145.4(13)
F21···F21$^{\mathrm{IV}}$–C1$^{\mathrm{IV}}$	157.9(7)	F22···F22$^{\mathrm{IX}}$–C1$^{\mathrm{X}}$	145.4(13)
C1–F21···F21$^{\mathrm{IV}}$–C1$^{\mathrm{IV}}$	180.0	C1–F22···F22$^{\mathrm{IX}}$–C1$^{\mathrm{X}}$	180.0
F21–F22$^{\mathrm{V}}$	2.66(3)		
C1–F21–F22$^{\mathrm{V}}$	122.4(11)		
F21–F22$^{\mathrm{V}}$–C1$^{\mathrm{V}}$	160.7(12)		
C1–F21–F22$^{\mathrm{V}}$–C1$^{\mathrm{V}}$	–108(7)		
F22···F21$^{\mathrm{VI}}$	2.66(3)		
C1–F22···F21$^{\mathrm{VI}}$	160.7(12)		
F22–F21$^{\mathrm{VI}}$–C1$^{\mathrm{VI}}$	122.4(11)		
C1–F22···F21$^{\mathrm{VI}}$–C1$^{\mathrm{VI}}$	108(7)		

Symmetry codes: (I) –*x*, –1/2 + *y*, 1/2 – *z*; (II) –*x*, 1/2 + *y*, 1/2 – *z*; (III) *x*, –*y*, –*z*; (IV) 1/2 – *x*, 1/2 – *y*, –*z*; (V) 1/2 – *x*, –1/2 + *y*, *z*; (VI) 1/2 – *x*, 1/2 + *y*, *z*; (VII) *x*, –*y*, *z*; (VIII) 1 – *x*, –*y*, –*z*; (IX) 1/2 – *x*, 1/2 – *y*,1 – *z*; (X) 1/2 – *x*, 1/2 + *y*, 1 – *z*.

Table S4. The dimensions (Å, °) of the intermolecular interactions in **3** and **4**.

Compound Temperature, K	**3** 185	**3** 100	Compound Temperature, K	**4** 160	**4** 100
I1···I1^{I}	3.8356(4)	3.7993(4)			
C2–I1···I1^{I}	102.26(11)	102.25(12)			
I1···I1^{I}–C2^{I}	177.82(11)	177.84(13)			
C2–I1···I1^{I}–C2^{I}	–158(3)	–163(3)			
I1···I1^{II}	3.8356(4)	3.7993(4)	I1···F1^{VI}	3.380(4)	3.334(4)
C2–I1···I1^{II}	177.82(11)	177.84(13)	C2–I1···F1^{VI}	155.55(13)	154.69(10)
I1···I1^{II}–C2^{II}	102.26(11)	102.25(12)	I1···F1^{VI}–C1^{VI}	156.5(6)	155.5(5)
C2–I1···I1^{II}–C2^{II}	158(3)	163(3)	C2–I1···F1^{VI}–C1^{VI}	180.0	180.0
F1···F2^{III}	2.864(3)	2.784(4)	F1···I1^{VII}	3.380(4)	3.334(4)
C1–F1···F2^{III}	157.3(3)	157.2(3)	C1–F1···I1^{VII}	156.5(6)	155.5(5)
F1···F2^{III}–C1^{III}	165.2(2)	164.9(3)	F1···I1^{VII}–C2^{VII}	155.55(13)	154.69(10)
C1–F1···F2^{III}–C1^{III}	159.8(12)	162.5(13)	C1–F1···I1^{VII}–C2^{VII}	180.0	180.0
F2···F1^{IV}	2.864(3)	2.784(4)			
C1–F2···F1^{IV}	165.2(2)	164.9(3)			
F2···F1^{IV}–C1^{IV}	157.3(3)	157.2(3)			
C1–F2···F1^{IV}–C1^{IV}	159.8(12)	162.5(13)			
F3···H21^{V}	2.72(3)	2.66(4)	F2···H4^{VIII}	2.64(2)	2.60(2)
C1–F3···H21^{V}	127(9)	125.5(12)	C1–F2···H4^{VIII}	137.7(8)	138.0(6)
F3···H21^{V}–C2^{V}	145(3)	144(4)	F2···H4^{VIII}–C4^{VIII}	144(2)	145.6(17)
C1–F3···H21^{V}–C2^{V}	64(6)	65(7)	C1–F2···H4^{VIII}–C4^{VIII}	–120(3)	–118(3)
H21···F3^{V}	2.72(3)	2.66(4)	H4···F2^{IX}	2.64(2)	2.60(2)
C2–H21···F3^{V}	145(3)	144(4)	C4–H4···F2^{IX}	144(2)	145.6(17)
H21···F3^{V}–C1^{V}	127(9)	125.5(12)	H4···F2^{IX}–C1^{X}	137.7(8)	138.0(6)
C2–H21···F3^{V}–C1^{V}	–64(6)	–65(7)	C4–H4···F2^{IX}–C1^{X}	120(3)	118(3)
			H2···C3	2.86(2)	2.83(2)
			C2–H2···C3	151.3(3)	150.8(3)
			H2···C3–C4	76.0(5)	75.9(5)
			H2···C3–C4^{XI}	76.1(5)	75.9(4)
			C2–H2···C3–C4	–119(4)	–120(4)
			C2–H2···C3–C4^{XI}	115(4)	114(4)
			H2···C3^{XII}	2.86(2)	2.83(2)
			C2–H2···C3^{XII}	151.3(3)	150.8(3)
			H2···C^{XII}–C4^{XII}	76.1(5)	75.9(4)
			H2···C3^{XII}–C4^{XIII}	76.0(5)	75.9(5)
			C2–H2···C3^{XII}–C4^{XII}	–115(4)	–114(4)
			C2–H2···C3^{XII}–C4^{XIII}	119(4)	120(4)
			H2···C4	2.85(3)	2.83(2)
			C2–H2···C4	152.1(17)	152.2(15)
			H2···C4–C3	76.2(4)	75.9(4)
			H2···C4–C4^{XIII}	76.13(15)	75.95(13)
			C2–H2···C4–C3	116(2)	115(2)
			C2–H2···C4–C4^{XIII}	–118(2)	–118(2)
			H2···C4^{XI}	2.86(2)	2.83(2)
			C2–H2···C4^{XI}	150.6(19)	149.6(17)
			H2···C4^{XI}–C3	76.1(5)	75.9(4)
			H2···C4^{XI}–C4^{XII}	76.14(11)	75.96(10)
			C2–H2···C4^{XI}–C3	–118(2)	–118.3(17)
			C2–H2···C4^{XI}–C4^{XII}	116(2)	115.2(19)
			H2···C4^{XIII}	2.85(3)	2.83(2)
			C2–H2···C4^{XIII}	152.1(17)	152.2(15)
			H2···C4^{XIII}–C4	76.13(15)	75.95(14)
			H2···C4^{XIII}–C3^{XII}	76.2(4)	75.9(4)
			C2–H2···C4^{XIII}–C4	118(2)	118(2)
			C2–H2···C4^{XIII}–C3^{XII}	–116(2)	–115(2)
			H2···C4^{XII}	2.86(2)	2.83(2)
			C2–H2···C4^{XII}	150.6(19)	149.6(17)
			H2···C4^{XII}–C3^{XII}	76.1(5)	75.9(4)
			H2···C4^{XII}–C4^{XI}	76.14(11)	75.96(10)
			C2–H2···C4^{XII}–C3^{XII}	117.7(19)	118.3(17)
			C2–H2···C4^{XII}–C4^{XI}	–116(2)	–115.2(19)

Symmetry codes: (I) 1/4 + *y*, 3/4 – *x*, 3/4 – *z*; (II) 3/4 – *y*, –1/4 + *x*, 3/4 – *z*; (III) –1/4 + *y*, 3/4 – *x*, 3/4 + *z*; (IV) 3/4 – *y*, 1/4 + *x*, –3/4 + *z*; (V) 1/2 – *x*, 1/2 – *y*, 3/2 – *z*; (VI) –1/2 + *x*, –1/2 + *y*, *z*; (VII) 1/2 + *x*, 1/2 + *y*, *z*; (VIII) –*x*, –1 + *y*, *z*; (IX) –*x*, 1 + *y*, *z*; (X) –*x*, 1 + *y*, 1/2 – *z*; (XI) *x*, 1 – *y*, 1 – *z*; (XII) –*x*, 1 – *y*, 1 – *z*; (XIII) –*x*, *y*, *z*.

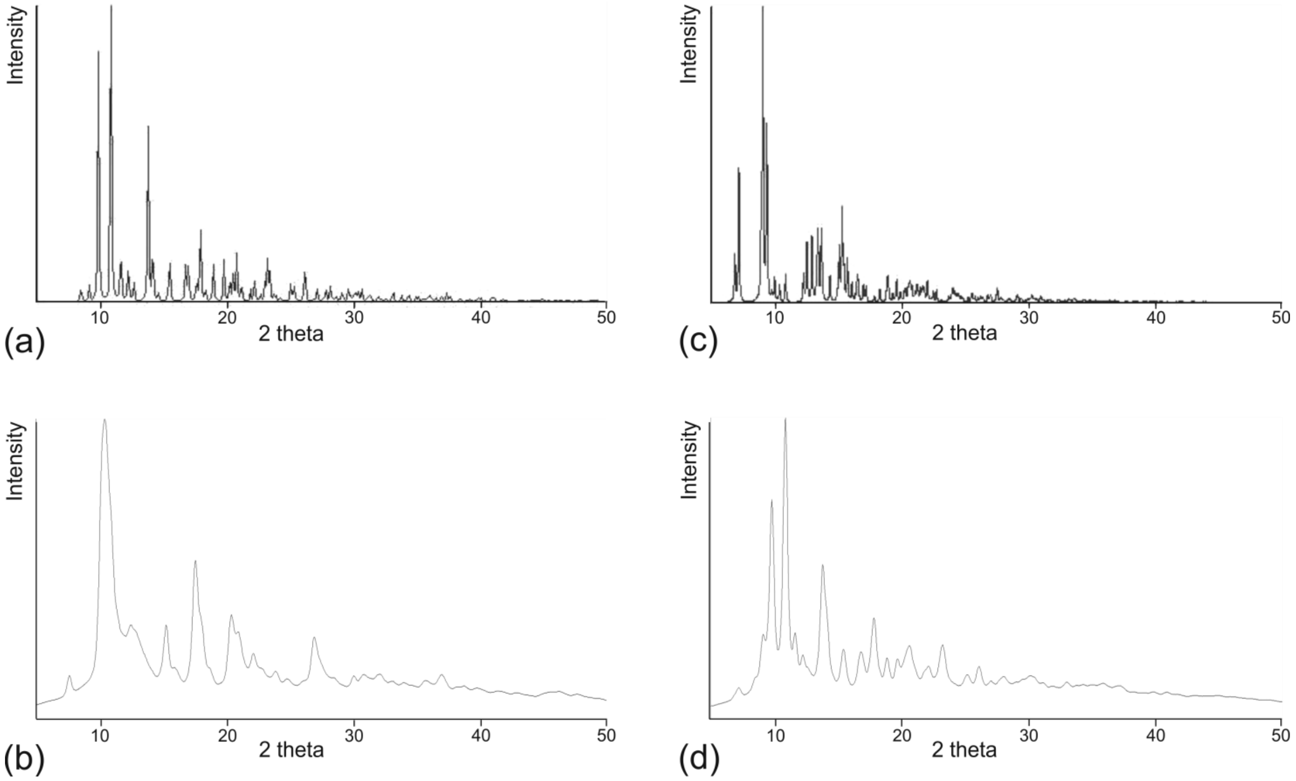

Figure S1. Simulated powder diffraction diagrams for the high-temperature phases of **1** at 120 K (a) and **2** at 140 K (c) along with experimental X-ray powder diffraction patterns for their low-temperature phases at 95 K (b) and 120 K (d), respectively.

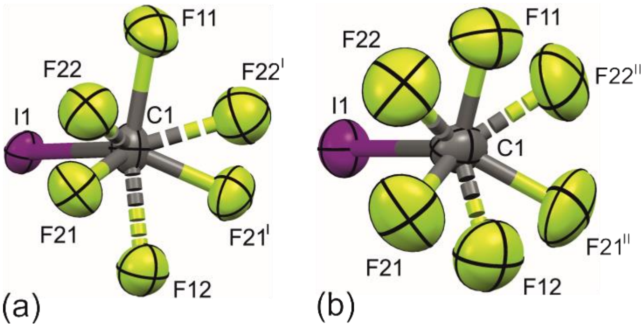

Figure S2. The disordered CF$_3$I molecules in the structures of **1** at 120 K (a) and **2** at 140 K (b). The refined occupation factors for two sites of the split –CF$_3$ groups: 78% (F11 and F21, solid line) and 22% (F12 and F22, dotted line) for **1**, and 65% (F11 and F21, solid line) and 35% (F12 and F22, dotted line) for **2**. Displacement ellipsoids are plotted at the 25% probability level. Symmetry codes: (I) *–x*, *y*, *z*; (II) *x*, *–y*, *z*

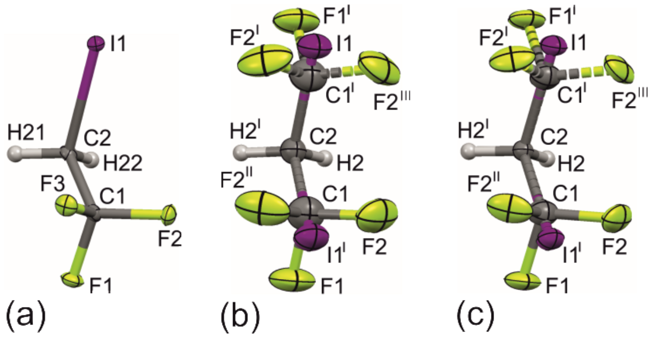

Figure S3. The CF$_3$CH$_2$I molecules: ordered in the structure of **3** at 100 K (a) and disordered in the structures of **4** at 160 K (b) and 100 K (c). Note the same *staggered* conformation for both ordered and disordered molecules. The solid and dotted lines were used to distinguish opposite orientations of the –CF$_3$ and –I substituents. Displacement ellipsoids are plotted at the 25% probability level. Symmetry codes: (I) *–x*, *y*, *–z* + 1/2; (II) *x*, *y*, *–z* + 1/2; (III) *–x*, *y*, *z*.

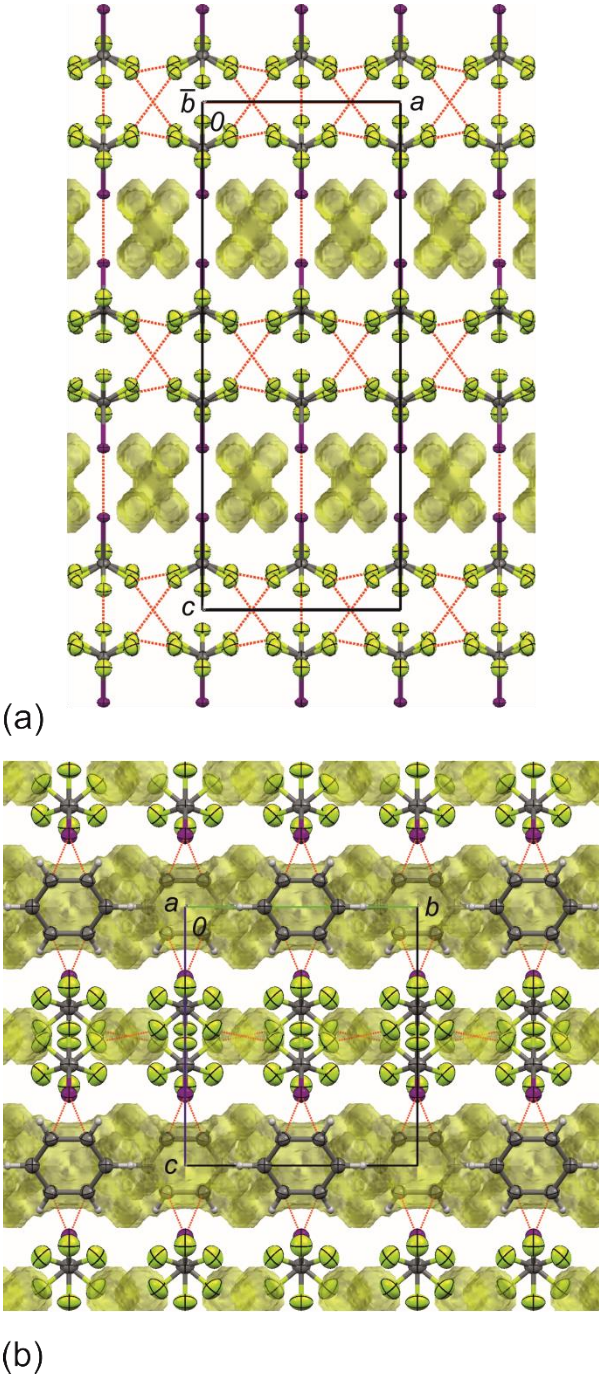

Figure S4. The structures of **1** at 120 K (a) and **2** at 140 K (b). The intermolecular space accessible to a probing sphere of radius 0.6 Å and grid size of 0.15 Å is indicated in yellow. The void volume is: 7.1% (60.27 Å^3) (a) and 12.4% (86.33 Å^3) (b), respectively.[5] The dotted red lines indicate the intermolecular interactions shorter than the sums of van der Waals radii.[13] Displacement ellipsoids are plotted at the 25% probability level.

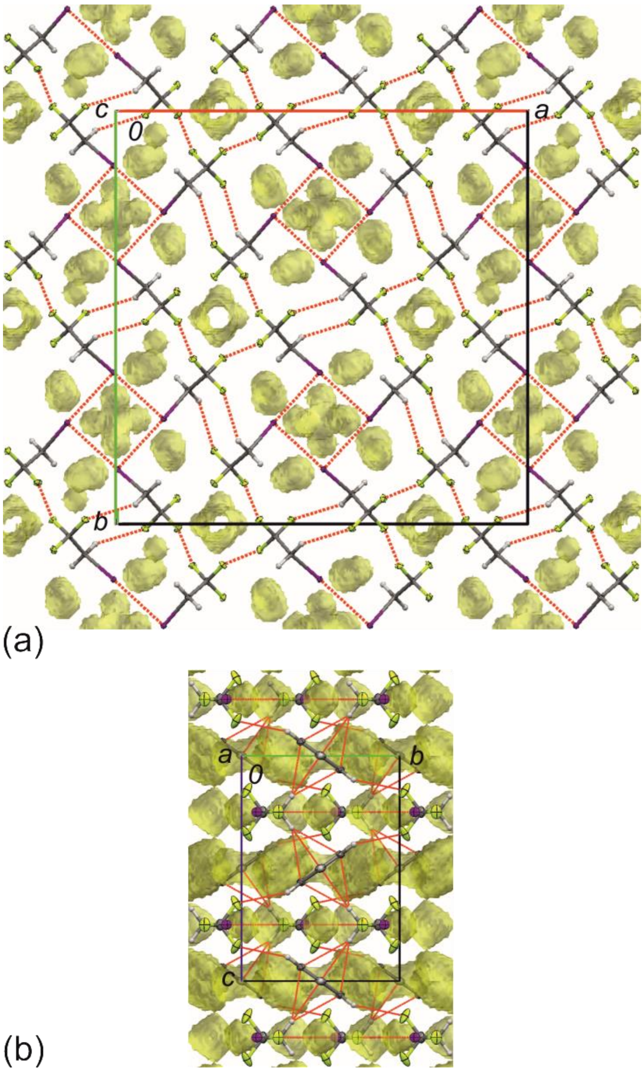

Figure S5. The structures, at 100 K, of **3** (a) and **4** (b). The intermolecular space accessible to a probing sphere of radius 0.6 Å and grid size of 0.15 Å is indicated in yellow. The void volume is: 7.3% (141.62 Å^3) (a) and 12.7% (129.59 Å^3) (b), respectively.[5] The dotted red lines indicate the intermolecular interactions shorter than the sums of van der Waals radii.[13] Displacement ellipsoids are plotted at the 25% probability level.

Table S5: Electronic energies of relevant species.

Molecule/complex		*E*/Hartree (M06-2X/def2TZVP)	*E*/Hartree (B2PLYP-D3/def2QZVP//M06-2X/def2TZVP)
C_6H_6		–232.2246242	–232.159948
F_3CI		–635.2963656	–635.2314031
F_3CCH_2I		–674.6203361	–674.5436027
$[F_3CI+C_6H_6]$		–867.5271678	–867.3983569
$[F_3CCH_2I+C_6H_6]$	H-bound	–906.8538267	–906.7117985
	I-bound	–906.8501701	–906.7096112
complexation energies, kJ·mol^{-1}			
$C_6H_6+F_3CI \rightarrow [C_6H_6+F_3CI]$		–16.2	–18.4
$C_6H_6+F_3CCH_2I \rightarrow [C_6H_6+F_3CCH_2I]$	H-bound	–23.3	–21.7
	I-bound	–13.7	–15.9

Table S6: SAPT0/def2TZVP energies of relevant species; all in kJ·mol^{-1}.

		$E_{\text{electrostatics}}$	E_{exchange}	$E_{\text{induction}}$	$E_{\text{dispersion}}$	E_{tot}
[F_3CI+C_6H_6]		−18.2	30.4	−7.1	27.1	−21.9
[F_3CCH_2I+C_6H_6]	H−bound	−24.7	39.9	−6.7	−34.7	−26.1
	I−bound	−15.0	29.3	−5.6	−26.8	−18.1
energy differences between H− and I−bound structures						
[C_6H_6+F_3CCH_2I]^{H} − [C_6H_6+F_3CCH_2I]^{I}		−9.6	10.6	−1.1	−7.9	−8.0

Table S7: NBO interactions between different components of the benzene π-system and the respective acceptor σ*-orbitals; all energies in kJ·mol^{-1}.

Interaction	A	B	[F_3CI+C_6H_6]	[F_3CCH_2I+C_6H_6]^{H}	[F_3CCH_2I+C_6H_6]^{I}
π(C_6H_6)→σ*(I-C)	C-C (1)	I-C	8.54		1.13
π(C_6H_6)→σ*(I-C)	C-C (2)	I-C	0.63		0.25
π(C_6H_6)→σ*(I-C)	C-C (3)	I-C	0.63		5.9
π(C_6H_6)→σ*(I-C)	C-C (4)	I-C			1.38
π(C_6H_6)→σ*(I-C)	C-C (5)	I-C			1.17
π(C_6H_6)→σ*(H-C)	C-C (1)	H-C (1)		1.13	
π(C_6H_6)→σ*(H-C)	C-C (1)	H-C (2)		0.59	
π(C_6H_6)→σ*(H-C)	C-C (2)	H-C (1)		2.05	
π(C_6H_6)→σ*(H-C)	C-C (3)	H-C (1)		1.34	

Table S8: Cartesian coordinates of C_6H_6, calculated at M06-2X/def2TZVP level of theory.

C	1.202408	0.694230	−0.000000
C	−0.000000	1.388428	−0.000000
C	−1.202408	0.694230	0.000000
C	−1.202408	−0.694230	0.000000
C	0.000000	−1.388428	0.000000
C	1.202408	−0.694230	−0.000000
H	2.139832	1.235421	−0.000000
H	0.000000	2.470877	−0.000000
H	−2.139832	1.235421	0.000000
H	−2.139832	−1.235421	0.000000
H	0.000000	−2.470877	−0.000000
H	2.139832	−1.235421	−0.000000

Table S9: Cartesian coordinates of F_3CI, calculated at M06-2X/def2TZVP level of theory.

C	0.271735	−1.141959	−0.000000
I	−0.223842	0.940867	0.000000
F	1.584705	−1.306541	−0.000000
F	−0.223842	−1.736408	1.073330
F	−0.223842	−1.736408	−1.073330

Table S10: Cartesian coordinates of F_3CCH_2I, calculated at M06-2X/def2TZVP level of theory.

I	−1.339415	−0.019752	−0.000000
F	1.707764	−0.784787	−1.077463
F	2.847463	0.691208	0.000004
F	1.707756	−0.784788	1.077463
C	0.540141	0.965575	−0.000002
C	1.698256	−0.000491	−0.000001
H	0.595872	1.580833	0.892196
H	0.595870	1.580834	−0.892199

Table S11: Cartesian coordinates of $[C_6H_6+F_3CI]$, calculated at M06-2X/def2TZVP level of theory.

I	−0.244226	0.494660	0.000000
C	0.194125	2.588785	0.000000
F	−0.922283	3.304828	0.000000
F	0.897509	2.924008	1.073392
F	0.897509	2.924008	−1.073392
C	−1.104759	−2.846001	0.695054
H	−2.038170	−2.758059	1.236239
C	0.094017	−2.955817	1.389401
H	0.094206	−2.951245	2.471659
C	1.290996	−3.065846	0.694454
H	2.224742	−3.147364	1.235451
C	1.290996	−3.065846	−0.694454
H	2.224742	−3.147364	−1.235451
C	0.094017	−2.955817	−1.389401
H	0.094206	−2.951245	−2.471659
C	−1.104759	−2.846001	−0.695054
H	−2.038170	−2.758059	−1.236239

Table S12: Cartesian coordinates of $[C_6H_6+F_3CCH_2I]^H$, calculated at M06-2X/def2TZVP level of theory.

C	0.518943	1.814017	–0.078308
F	–0.372956	2.678270	–0.586718
F	0.265360	1.706822	1.226764
C	0.412033	0.501351	–0.811160
H	–0.601500	0.120927	–0.725620
I	1.720407	–0.971472	–0.023515
H	0.678873	0.661512	–1.850916
F	1.724951	2.371592	–0.208805
C	–2.027721	–1.688362	0.667147
H	–1.531002	–2.554327	1.084748
C	–2.560806	–1.743476	–0.614821
H	–2.485317	–2.655242	–1.193222
C	–2.118189	–0.516090	1.406792
H	–1.687740	–0.467258	2.398573
C	–3.281279	0.544529	–0.413820
H	–3.763910	1.416317	–0.836153
C	–2.744980	0.600010	0.866435
H	–2.803074	1.516948	1.438430
C	–3.188151	–0.627142	–1.155075
H	–3.603180	–0.670030	–2.153867

Table S13: Cartesian coordinates of $[C_6H_6{+}F_3CCH_2I]^I$, calculated at M06-2X/def2TZVP level of theory.

I	0.154352	–0.418043	0.010385
F	3.164761	0.177023	1.292848
F	2.834941	1.522757	–0.357661
F	4.357594	0.006130	–0.491585
C	–3.430977	–1.053070	0.384272
C	–3.489958	0.690660	–1.271256
C	–3.642690	–0.645741	–0.926260
C	–3.125359	1.620378	–0.306585
C	–3.067558	–0.122933	1.350794
C	–2.913438	1.214098	1.004413
C	2.152862	–0.722827	–0.645571
C	3.119806	0.259825	–0.037430
H	–3.545165	–2.095333	0.652972
H	–3.650965	1.007261	–2.293603
H	–3.922319	–1.370949	–1.679404
H	–3.000248	2.660790	–0.576884
H	–2.899293	–0.440603	2.371907
H	2.453159	–1.726754	–0.362680
H	2.175672	–0.611018	–1.724966
H	–2.623271	1.937359	1.755545

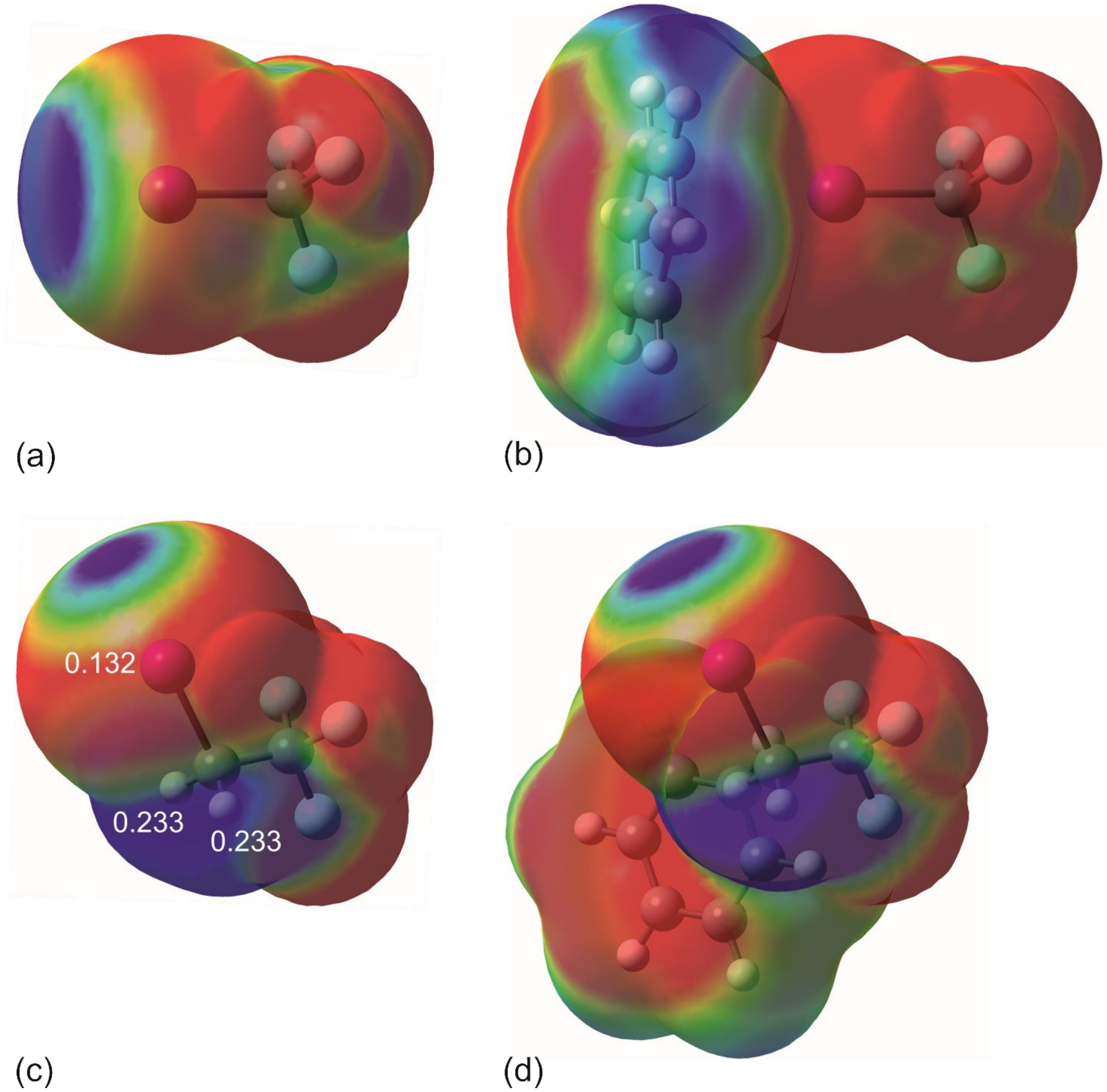

Figure S6. The molecular isodensity surfaces of **1** (a), **2** (b), **3** (c) and **4** (d) mapped with their electrostatic potential. The colours show positive from 0.02 a.u. (blue) to negative –0.002 a.u (red) and intermediate degrees (orange-green) of electrostatic potential. The calculated partial atomic charges (NBO), for the positive sites of I and H atoms in **3**, are also provided.

References

[1] a) G. E. Bacon, N. A. Curry, S. A. Wilson, *Proc. R. Soc. London, Ser. A* **1964**, *279*, 98; b) M. Woińska, S. Grabowsky, P. M. Dominiak, K. Woźniak, D. Jayatilaka, *Sci. Adv.* **2016**, *2*, e1600192.

[2] *e.g.* a) M. A. Viswamitra, K. K. Kannan, *Nature* **1966**, *209*, 1016; b) D. Brodalla, D. Mootz, R. Boese, W. Osswald, *J. Appl. Cryst.* **1985**, *18*, 316; c) M. T. Kirchner, D. Bläser, R. Boese, *Chem. Eur. J.* **2010**, *16*, 2131; d) A. E. Goeta, J. A. K. Howard, *Chem. Soc. Rev.* **2004**, *33*, 490; e) M. Bujak, M. Podsiadło, A. Katrusiak, *J. Phys. Chem. B* **2008**, *112*, 1184; f) R. Boese, *Z. Kristallogr.* **2014**, *229*, 595; g) D. Li, J. Schwabedissen, H.-G. Stammler, N. W. Mitzel, H. Willner, X. Zeng, *Phys. Chem. Chem. Phys.* **2016**, *18*, 26245.

[3] CrysAlisPro, Rigaku Oxford Diffraction, version 1.171.39.15e, Rigaku Corporation, The Woodlands TX, **2015**.

[4] a) G. M. Sheldrick, *Acta Crystallogr. Sect. A* **2008**, *64*, 112; b) G. M. Sheldrick, *Acta Crystallogr. Sect. C* **2015**, *71*, 3.

[5] C. F. Macrae, I. J. Bruno, J. A. Chisholm, P. R. Edgington, P. McCabe, E. Pidcock, L. Rodriguez−Monge, R. Taylor, J. van de Streek, P. A. Wood, *J. Appl. Crystallogr.* **2008**, *41*, 466.

[6] a) S. K. Wolff, D. J. Grimwood, J. J. McKinnon, D. Jayatilaka, M. A. Spackman, CrystalExplorer 2.0. University of Western Australia, Crowley, Australia, **2007**; b) J. J. McKinnon, M. A. Spackman, A. S. Mitchell, *Acta Crystallogr. Sect. B* **2004**, *60*, 627; c) M. A. Spackman, J. J. McKinnon, D. Jayatilaka, *CrystEngComm* **2008**, *10* 377; d) M. A. Spackman, D. Jayatilaka, *CrystEngComm* **2009**, *11*, 19.

[7] M. J. Frisch, G. W. Trucks, H. B. Schlegel, G. E. Scuseria, M. A. Robb, J. R. Cheeseman, G. Scalmani, V. Barone, B. Mennucci, G. A. Petersson, H. Nakatsuji, M. Caricato, X. Li, H. P. Hratchian, A. F. Izmaylov, J. Bloino, G. Zheng, J. L. Sonnenberg, M. Hada, M. Ehara, K. Toyota, R. Fukuda, J. Hasegawa, M. Ishida, T. Nakajima, Y. Honda, O. Kitao, H. Nakai, T. Vreven, J. A. Montgomery, Jr., J. E. Peralta, F. Ogliaro, M. Bearpark, J. J. Heyd, E. Brothers, K. N. Kudin, V. N. Staroverov, R. Kobayashi, J. Normand, K. Raghavachari, A. Rendell, J. C. Burant, S. S. Iyengar, J. Tomasi, M. Cossi, N. Rega, J. M. Millam, M. Klene, J. E. Knox, J. B. Cross, V. Bakken, C. Adamo, J. Jaramillo, R. Gomperts, R. E. Stratmann, O. Yazyev, A. J. Austin, R. Cammi, C. Pomelli, J. W. Ochterski, R. L. Martin, K. Morokuma, V. G. Zakrzewski, G. A. Voth, P. Salvador, J. J. Dannenberg, S. Dapprich, A. D. Daniels, O. Farkas, J. B. Foresman, J. V. Ortiz, J. Cioslowski, D. J. Fox, Gaussian 09, Revision A.02, Gaussian, Inc., Wallingford CT, **2009**.

[8] R. Dennington, T. Keith, J. Millam, GaussView 5.0, Semichem Inc., Shawnee Mission, KS, **2009**.

[9] A. D. Becke, *Phys. Rev. A* **1988**, *38*, 3098.

[10] C. Lee, W. Yang, R. G. Parr, *Phys. Rev. B* **1988**, *37*, 785.

[11] R. Krishnan, J. S. Binkley, R. Seeger, J. A. Pople, *J. Chem. Phys.* **1980**, *72*, 650.

[12] M. N. Glukhovstev, A. Pross, M. P. McGrath, L. Radom, *J. Chem. Phys.* **1995**, *103*, 1878.

[13] a) A. Bondi, *J. Phys. Chem.* **1964**, *68*, 441; b) S. C. Nyburg, C. H. Faerman, *Acta Crystallogr. Sect. B* **1985**, *41*, 274; c) S. S. Batsanov, *Inorg. Mater.* **2001**, *37*, 871; d) S.−Z. Hu, Z.−H. Zhou, Z.−X. Xie, B. E. Robertson, *Z. Kristallogr.* **2014**, *229*, 517.

[14] S. Grimme, C. Bannwarth, P. Shushkov, *J. Chem. Theory. Comput.*, **2017**, *13*, 1989.

[15] Gaussian 16, Revision B.01, M. J. Frisch, G. W. Trucks, H. B. Schlegel, G. E. Scuseria, M. A. Robb, J. R. Cheeseman, G. Scalmani, V. Barone, G. A. Petersson, H. Nakatsuji, X. Li, M. Caricato, A. V. Marenich, J. Bloino, B. G. Janesko, R. Gomperts, B. Mennucci, H. P. Hratchian, J. V. Ortiz, A. F. Izmaylov, J. L. Sonnenberg, D. Williams-Young, F. Ding, F. Lipparini, F. Egidi, J. Goings, B. Peng, A. Petrone, T. Henderson, D. Ranasinghe, V. G. Zakrzewski, J. Gao, N. Rega, G. Zheng, W. Liang, M. Hada, M. Ehara, K. Toyota, R. Fukuda, J. Hasegawa, M. Ishida, T. Nakajima, Y. Honda, O. Kitao, H. Nakai, T. Vreven, K. Throssell, J. A. Montgomery, Jr., J. E. Peralta, F. Ogliaro, M. J. Bearpark, J. J. Heyd, E. N. Brothers, K. N. Kudin, V. N. Staroverov, T. A. Keith, R. Kobayashi, J. Normand, K. Raghavachari, A. P. Rendell, J. C. Burant, S. S. Iyengar, J. Tomasi, M. Cossi, J. M. Millam, M. Klene, C. Adamo, R. Cammi, J. W. Ochterski, R. L. Martin, K. Morokuma, O. Farkas, J. B. Foresman, D. J. Fox, Gaussian, Inc., Wallingford CT, **2016**.

[16] NBO Version 3.1, E. D. Glendening, A. E. Reed, J. E. Carpenter, F. Weinhold.

[17] R. M. Parrish, L. A. Burns, D. G. A. Smith, A. C. Simmonett, A. E. DePrince III, E. G. Hohenstein, U. Bozkaya, A. Yu. Sokolov, R. Di Remigio, R. M. Richard, J. F. Gonthier, A. M. James, H. R. McAlexander, A. Kumar, M. Saitow, X. Wang, B. P. Pritchard, P. Verma, H. F. Schaefer III, K. Patkowski, R. A. King, E. F. Valeev, F. A. Evangelista, J. M. Turney, T. D. Crawford, C. D. Sherrill, *J. Chem. Theory Comput.*, **2017**, *13*, 3185.